Universal phonon softening in the pseudogap state of $Tl_2Ba_2Ca_{n-1}Cu_nO_{2n+4+\delta}$

Jia-Wei Hu,[1,2,3] Kai Zhang,[3] Yong-Chang Ma,[4] Nan-Lin Wang,[5] Viktor V. Struzhkin,[3] Alexander F. Goncharov,[6] Hai-Qing Lin,[7] and Xiao-Jia Chen[8,*]

[1]*Key Laboratory of Materials Physics, Institute of Solid State Physics, HFIPS, Chinese Academy of Sciences, Hefei 230031, China*
[2]*University of Science and Technology of China, Hefei 230026, China*
[3]*Center for High Pressure Science and Technology Advanced Research, Shanghai 201203, China*
[4]*School of Materials Science and Engineering, Tianjin University of Technology, Tianjin 300384, China*
[5]*International Center for Quantum Materials, School of Physics, Peking University, Beijing 100871, China*
[6]*Earth and Planets Laboratory, Carnegie Institution for Science, Washington, DC 20015, USA*
[7]*School of Physics, Zhejiang University, Hangzhou 310058, China*
[8]*Department of Physics and TcSUH, University of Houston, Houston, Texas 77204, USA*

(Received 11 April 2023; revised 6 June 2023; accepted 7 June 2023; published 15 June 2023)

Exploring the origin of the pseudogap is important for the understanding of superconductivity in cuprates. Here we report a systematical experimental study on the phonon vibrational properties of $Tl_2Ba_2Ca_{n-1}Cu_nO_{2n+4+\delta}$ ($n = 1, 2, 3$) single crystals based on the Raman scattering measurements over the temperature range from 10–300 K. The temperature evolution of the frequency and linewidth of the observed phonon modes in each member of this family does not follow the expected self-energy effect when entering the superconducting state. The anomalies are observed for the phonon modes involving the vibrations of the atoms in the Tl-O layer and the apical oxygen at the temperature around 150 K, which is higher above the superconducting transition. The phonon mode of the apical oxygen exhibits a pronounced universal softening behavior. From the comparison with the existing experimental data for various orders, we find that the observed starting temperature for the phonon softening corresponds to the onset opening temperature of the pseudogap. This finding indicates a large lattice effect in the pseudogap state and the non-negligible spin-phonon coupling for such a phonon softening.

DOI: 10.1103/PhysRevB.107.224508

I. INTRODUCTION

The pseudogap has been widely investigated in cuprate superconductors [1,2]. Its origin and connection to the superconducting gap are two key issues in the understanding of the mechanism of the superconductivity in cuprates. The spectroscopic evidence was given for a pseudogap in the normal state of underdoped $Bi_2Sr_2CaCu_2O_{8+\delta}$ by using angle-resolved photoemission spectroscopy (ARPES) [3]. The pseudogap was found to have the similar d-wave symmetry as the superconducting gap in the underdoped regime [3]. Similar observations were reported in single layer $Bi_2Sr_{2-x}La_xCuO_{6+\delta}$ [4]. Further work on underdoped $La_{2-x}Sr_xCuO_4$ showed that the opening of the pseudogap and the superconducting gap occur with almost the same energy scale [5]. All these phenomena suggested a precursor pairing of the electrons in the pseudogap state [6–8]. Notably, the evidence for decoupling of the pseudogap state from the superconducting state was also reported [9,10]. For example, the pseudogap state was found along with a particle-hole asymmetry in $Pb_{0.55}Bi_{1.5}Sr_{1.6}La_{0.4}CuO_{6+\delta}$ and $Bi_2Sr_2CaCu_2O_{8+\delta}$ [9,10], which was distinct from superconducting state. Recently, the spin textures in the pseudogap state of $YBa_2Cu_3O_{6+x}$ have been observed at the nanometer scale [11], supporting the magnetic order characterizing the pseudogap phase in cuprates reported previously [12,13]. Meanwhile, ARPES measurements revealed that the pseudogap exhibits an antagonistic behavior near the superconducting transition temperature T_c [14]. This behavior classifies the pseudogap as a competing order similar to other competing phases [15–17]. In fact, the time-reversal symmetry has been observed to break spontaneously just below the opening temperature of the pseudogap [18], indicating a phase transition takes place there.

So far, no consensus has been reached for explaining such complex competitive or cooperative behaviors. One of the well-known scenarios is the spin-charge separation based on the resonating-valence-bond model [19]. Within this framework, the pseudogap state is assumed to be a spin-liquid state without the long-range order. The spinons pair, which originates from the separation between the spin and charge, forms a spin-excitation gap (pseudogap) [1,20]. Extensive experiments based on Raman scattering spectroscopy have revealed that the two-magnon peak energy evolves with doping in a similar manner as the pseudogap and pair peak in almost all cuprate superconductors [21–23]. These similarities indicate that the high-energy magnetic fluctuations are directly involved in the formation of the pseudogap and the Cooper pairing interaction. Such a coupling from the high-

*xjchen@uh.edu

 ©2023 American Physical Society

energy excitation to superconducting quasiparticles has been captured from coherent charge fluctuation spectroscopy [24]. Numerical computation clearly reproduced the two-magnon peak and its gradual development to a quasiparticle response with doping [25]. Although the magnetic signature for the pseudogap as well as the magnetic origin for the superconductivity have been indicated from experiments and theory [11–13,21–25], some non-negligible lattice effect on the pseudogap state has also been reported [26–28]. For instance, upon oxygen isotope substitution (^{16}O / ^{18}O), the onset temperature of the pseudogap remarkably shifts in $La_{2-x}Sr_xCuO_4$ [26] and $HoBa_2Cu_4O_8$ [27]. The huge oxygen isotope effects indicate a strong electron-phonon interaction for the pseudogap formation.

$Tl_2Ba_2Ca_{n-1}Cu_nO_{2n+4+\delta}$ [abbreviated as Tl-22$(n-1)n$] ($n = 1, 2, 3$) superconductors have attracted significant interest because of their high T_c's (>90 K) at ambient pressure [29,30]. Such high T_c's allow the study of the physical properties in the superconducting and normal state over a wide temperature range. The investigations on the homogeneous layered family have been proven to be powerful and effective to draw important information such as lattice effect on superconductivity in cuprates [31–33]. The crystal structures of Tl-based superconductors have common features with the other high-T_c superconductors [34–38]. Much effort has been devoted to study the normal and superconducting state of Tl-based superconductors [39–46]. In particular, Raman scattering at low-temperatures can probe both phonon and electronic states as well as their interaction near the Fermi surface [47–54]. The vibrational modes are sensitive to the structure and symmetry change. The possible concerns such as defects and the impurity effects can be safely removed by using high-quality single crystals. Therefore, the Raman scattering spectroscopy has been widely used to study many important physical properties of cuprates such as the superconducting gap [55–62], energy scales [21–23,63], Cooper-pair density [64], charge density wave [65,66], pseudogap [67–70], and superconducting fluctuations [67], etc. Currently, the Raman measurements concentrated on the physics in the pseudogap regime of Tl-based family are still missing but desired.

To address all the above-mentioned issues, we perform systematic Raman scattering measurements on $Tl_2Ba_2Ca_{n-1}Cu_nO_{2n+4+\delta}$ ($n = 1, 2, 3$) single crystals at the interesting temperature range. The collected phonon modes are carefully analyzed by using the Fano profile. The obtained frequency and linewidth of each phonon mode allow us to establish a connection among various orders. Their temperature-dependent behaviors are discussed and the possible origin of the pseudogap state is given based on the observations.

II. EXPERIMENTAL DETAILS

The single-phase Tl-based crystals synthesized by flux method were detailed previously [71]. Tl-2201, Tl-2212, and Tl-2223 crystals have body-centered tetragonal lattice with $I4/mmm$ space group. Furthermore, no other phases could be detected from the diffraction patterns. Each sample has a good c-axial orientation, which is perpendicular to the sample's natural growth surface. The magnetic susceptibility measurements were used to determine the superconducting transition for the Tl-2201, Tl-2212, and Tl-2223 sample at temperature of 92, 109, and 119 K, respectively [71,72].

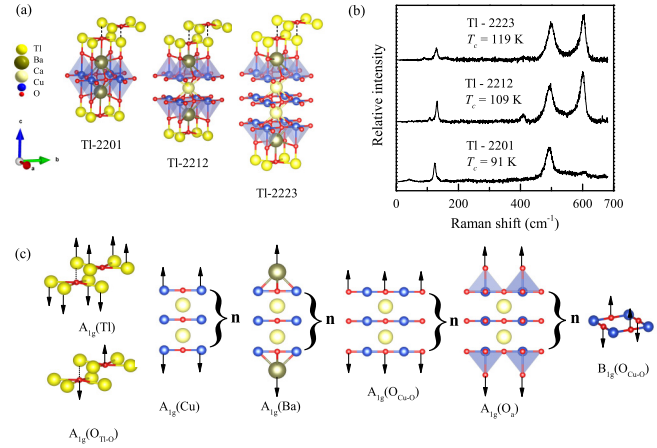

FIG. 1. (a) Tetragonal structure ($I4/mmm$) of $Tl_2Ba_2Ca_{n-1}Cu_nO_{2n+4+\delta}$ ($n = 1, 2, 3$). (b) The representative Raman spectra of Tl-2201, Tl-2212, and Tl-2223 collected with the 488 nm wavelength excitation at room temperature. The T_c value is taken from the susceptibility measurements. (c) The symmetry of the phonon vibrational modes observed experimentally in Tl-based system. The arrows show the direction of the vibrational modes.

The parallelepiped-shaped, as-grown samples have been cleaved into a size of $100 \times 100 \times 20$ μm ^{3} with a smooth surface and their c axis along the thinnest dimension. All the prepared samples were fixed with liquid adhesive in a cryogenic vacuum chamber. Raman spectra were measured with the z(x′y′$\bar{z}$) polarization in a near-backscattering geometry. A 488 nm laser was used to excite the Raman response. The laser power was kept at 1.5 mW to reduce the heating effect. An 1800 g/mm grating was used to obtain the spectra. The scattered light was recorded with a charge-coupled device designed by Princeton Instruments (PIX100BRX-SF-Q-F-A). A continuous flow cryostat with a high vacuum (6.1×10^{-7} mbar) was used for controlling the sample temperature from 10 K to room temperature.

III. RESULTS

A. Assignment of the Raman modes

The crystal structure of $Tl_2Ba_2Ca_{n-1}Cu_nO_{2n+4+\delta}$ ($n = 1, 2, 3$) is shown in Fig. 1(a). To classify the lattice vibrations and combine them with the theoretical shell model, we consider the space group $I4/mmm$ as the symmetry in layered copper oxides. The structures differ from each other by the number of consecutive CuO_2 layers. The corner sharing square-planar CuO_4 group is oriented parallel to the c direction. The individual CuO_2 layer is separated by the Ca atom. There are also two rocksalt type Tl-O layers in this structure giving a layer repeating sequence of [Tl-Ba-Cu-Ca-Cu-Ba-Tl]$_n$ along the c direction.

Figure 1(b) shows a complete set of Raman spectra of Tl-based compounds measured using the 488 nm laser line at room temperature. All Tl-based crystals have only atoms at

TABLE I. The irreducible representations of the Raman active modes and phonon assignments of $Tl_2Ba_2Ca_{n-1}Cu_nO_{2n+4+\delta}$ ($n = 1, 2, 3$). The frequencies are expressed in cm^{-1}. The literature data are from the works of Kulkarn *et al.* [73,74] and McCarty *et al.* [75,76] as listed in parentheses.

Sample	Raman-active irreducible	A_{1g}(Ba)	A_{1g}(Tl)	A_{1g}(Cu)	$B_{1g}(O_{Cu-O})$	$A_{1g}(O_{Cu-O})$	$A_{1g}(O_a)$	$A_{1g}(O_{Tl-O})$
$Tl-2201$	$4A_{1g}+4E_g$	124	162	–	–	–	491	603
		(122)	(167)	–	–	–	(495)	(612)
$Tl-2212$	$6A_{1g}+7E_g+B_{1g}$	107	133	161	–	410	494	602
		(108)	(130)	(158)	–	(407)	(494)	(599)
$Tl-2223$	$7A_{1g}+8E_g+B_{1g}$	90	132	161	269	403	501	608
		(99)	(133)	(159)	(275)	(405)	(498)	(601)

positions with site symmetry D_{4h}, D_{2h}, C_{4v}, and C_{2v}. Strong peaks show up in the $z(x'y')\bar{z}$ polarization. The spectra contain phonons with the $A_{1g}+B_{1g}$ symmetry. The prominent features are located at 124, 162, 491, and 603 cm^{-1} for Tl-2201, at 107, 133, 161, 410, 494, and 602 cm^{-1} for Tl-2212, and at 90, 132, 161, 269, 403, 501, and 608 cm^{-1} for Tl-2223. Table I gives a list of the Raman-active irreducible modes and the phonon mode assignment for $Tl_2Ba_2Ca_{n-1}Cu_nO_{2n+4+\delta}$. The obtained results are generally consistent with the earlier studies [73–77].

In Fig. 1(c), we show the suggested eigenvector patterns corresponding to the eigenmodes of A_{1g} symmetry and B_{1g} symmetry for the Tl-based compounds. However, the B_{1g} mode of the oxygen ions in the Cu-O planes is hard to be detected in the measurements. Early Raman spectroscopy studies on Tl-based samples also reported the absence of such B_{1g} phonon branches [39,73–77]. The relatively low Raman activity of the B_{1g} modes in Tl-based system was interpreted due to the relatively small perturbations [39] in their more uniform structures [37].

B. Temperature dependence of the Raman spectra

Figures 2(a)–2(c) show the spectrum mappings in the entire studied temperature range, where the red color represents the high scattering intensity and the blue color represents the low intensity. It can be clearly seen that there is a significant red shift for the A_{1g}(Tl), $A_{1g}(O_a)$, and $A_{1g}(O_{Tl-O})$ mode in the low-temperature region. As shown in Figs. 2(d)–2(f), the line shape of the phonon modes at representative temperatures exhibits an asymmetric Fano resonance behavior. Quantitative analysis of the linewidth and frequency of these modes was carried out by fitting the line shapes to the Fano profile [53] with a linear background,

$$I(\omega) = I_0\frac{(q+\epsilon)^2}{1+\epsilon^2} + \text{background}, \tag{1}$$

where

$$\epsilon = \frac{(\omega-\omega_0)}{\gamma}. \tag{2}$$

Here, I_0 is the relative intensity of the phonon peak, ω and ω_0 are the experimental and resonance frequency, 2γ is the full width at the half-maximum, and q is the asymmetric factor of the phonon shape.

Typical spectra of the $A_{1g}(O_a)$ mode in Tl-2201 between 10 and 300 K are shown in Fig. 3(a). The peaks display asymmetric line shapes which suggest an interaction between these discrete phonon states and a broad electronic continuum. The values of ω, γ, and q as a function of temperature are given in Fig. 3(b). At temperatures above 150 K, an overall ω softening, a linewidth narrowing, and a small increase of q can be seen around T_c (red dot lines) when going from the normal to superconducting state. The ω value shifts downward by 2 cm^{-1} in the temperature range between 150 and 92 K. The accompanying linewidth narrowing in the same temperature range is about 1 cm^{-1}, just above the instrument detection limit. The line-shape parameter q fluctuates below T_c. The peak position of the A_{1g} mode exhibits an obvious phonon softening far above T_c. However, the γ remains almost unchanged in the temperature range of 10–150 K.

C. Phonon mode analysis

The behaviors of ω and γ for $Tl_2Ba_2Ca_{n-1}Cu_nO_{2n+4+\delta}$ ($n = 1, 2, 3$) as a function of temperature are shown in Figs. 4–6, respectively. It is found that the A_{1g}(Tl) mode in each member of this family shifts to higher frequencies on cooling from temperature of 300–150 K, followed by a shift back to lower frequencies on cooling through T_c (Fig. 4). The peak position increases from 162 (at 300 K) to 168 cm^{-1} (at 150 K) for Tl-2201, 131 (at 300 K) to 135 cm^{-1} (at 150 K) for Tl-2212, and 132 (at 300 K) to 133 cm^{-1} (at 150 K) for Tl-2223, respectively. The accompanying γ narrowing during the whole temperature range is nearly 1–2 cm^{-1}. All three curves for the peak position of the A_{1g}(Tl) mode are similar demonstrating a maximum above T_c, softening on cooling down to T_c and then nearly constant in superconducting state. The data agree with the early report for Tl-2201, Tl-2212, and Tl-2223 [46] but disagree with those for the single-layer and bilayer samples [39]. Comparing with the Y-based and Bi-based cuprate superconductors [50,68], the low-frequency A_{1g} modes in the Tl-based system exhibit a mode-hardening behavior at low temperatures.

The temperature dependence of the apical oxygen $A_{1g}(O_a)$ mode of the Tl-based compounds observed at around

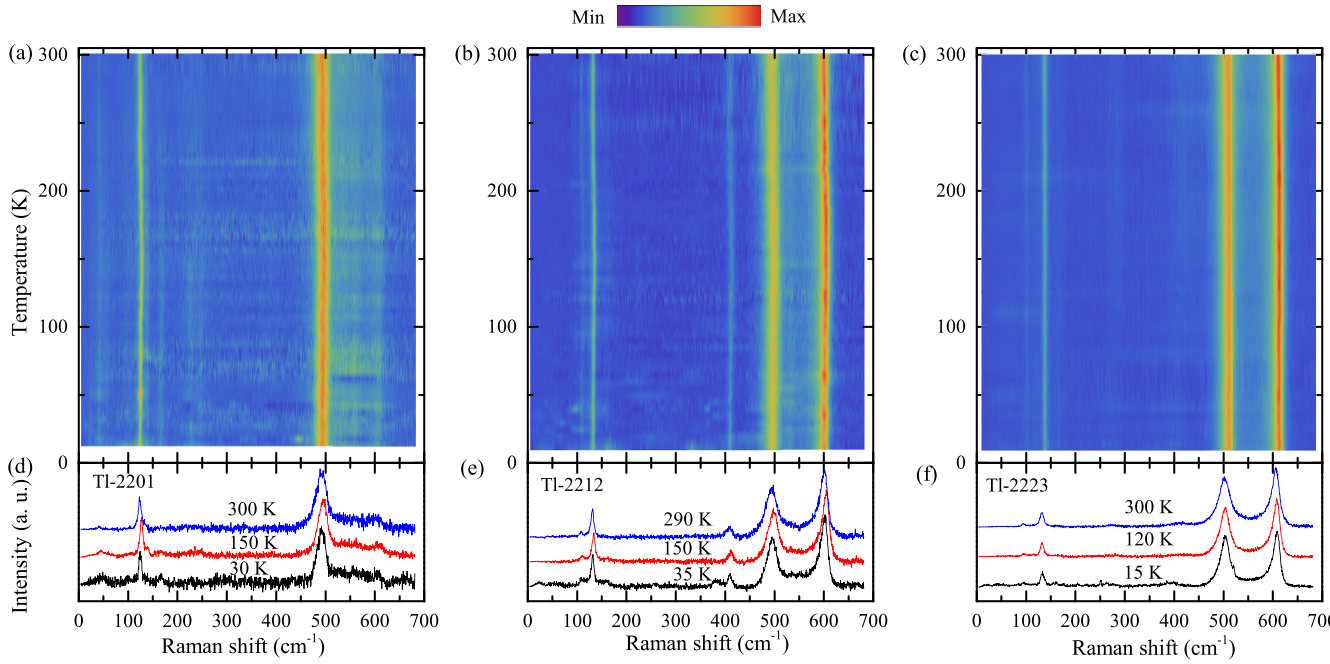

FIG. 2. Temperature-dependent Raman active modes. (a)–(c) The mapping graph for Tl-2201, Tl-2212, and Tl-2223, where the red color indicates the high intensity, while the blue color indicates the low intensity. The data points are normalized with respect to the peak value to show the trends of the frequency and width of the phonon peak. (e)–(f) Typical Raman spectra of $Tl_2Ba_2Ca_{n-1}Cu_nO_{2n+4+\delta}$ ($n = 1, 2, 3$) excited by a 488 nm laser at selected temperatures.

500 cm^{-1} is shown in Fig. 5. Similar to the A_{1g}(Tl) mode, all the frequencies show a monotonic increase over 150 K. For Tl-2201 and Tl-2212, ω downshifts by 3–4 cm^{-1} below T_c, and Tl-2223 exibits softening by about 1 cm^{-1} in the superconducting state. Meanwhile, the γ value is reduced by 2.5 cm^{-1} for Tl-2201, 3 cm^{-1} for Tl-2212, and 4 cm^{-1} for Tl-2223 from 300–10 K. Phonon anomalies were observed in the previous Raman studies for the apical oxygen modes [44–46]. The $A_{1g}(O_a)$ mode for the studied Tl-2201, Tl-2212, and Tl-2223 shows a softening behavior at temperature below 150 K but above T_c of each member of this layered family. For comparison, the phonon softening was also found at temperature below T_c in $HgBa_2Ca_2Cu_3O_{8+\delta}$ and $Bi_2Sr_2CaCu_2O_{8+\delta}$ [48,49,51]. It should be noticed that Tl-based samples exhibit a frequency softening for the apical oxygen model at high temperature above the T_c value.

The $A_{1g}(O_{Tl-O})$ mode in the charge reservoir layer of the Tl-based materials shows softening again in the frequency across 150 K (Fig. 6). Clearly, phonon softening is about 8 cm^{-1} for Tl-2201, 2 cm^{-1} for Tl-2212, and 1 cm^{-1} for

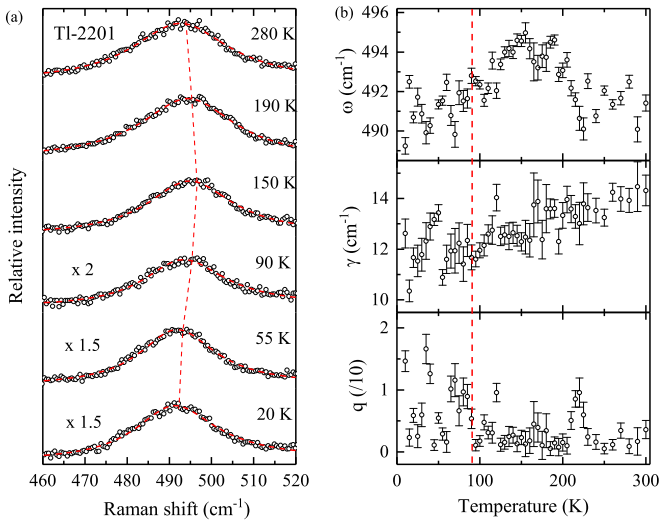

FIG. 3. (a) Representative Raman spectra (the black open circle) of Tl-2201 and the Fano fitting curve (red dash line) of the $A_{1g}(O_a)$ mode. The dashed curve indicates the frequency shift with temperature. (b) Temperature dependence of the ω, γ, and q value. The error bars correspond to uncertainties in determining these parameters. The red vertical dashed line represents the T_c value.

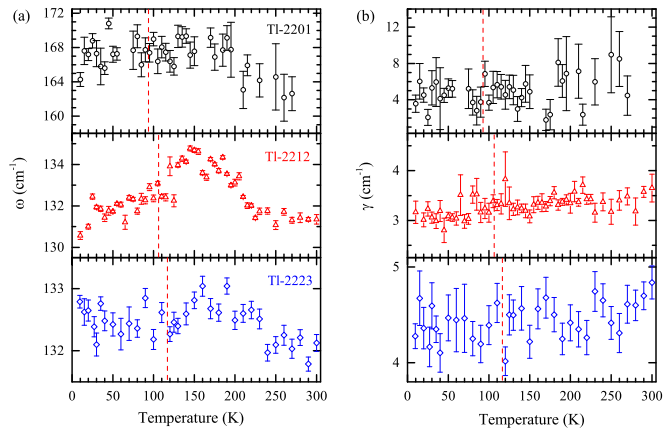

FIG. 4. Temperature dependence of the (a) ω and (b) γ of the A_{1g} (Tl) mode in Tl-2201 (black symbols), Tl-2212 (red symbols), and Tl-2223 (blue symbols). The red vertical dashed line represents the corresponding T_c.

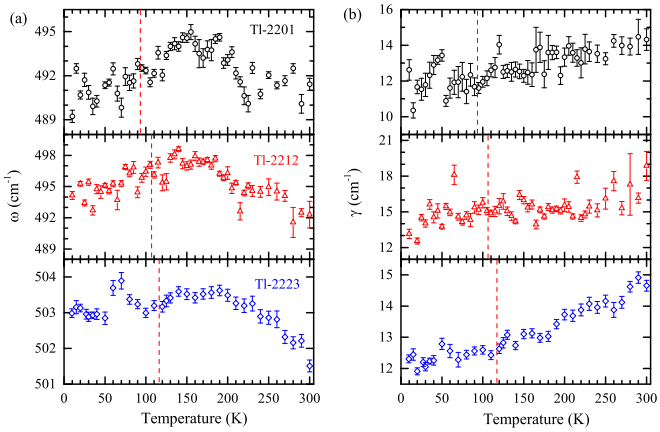

FIG. 5. Temperature dependence of the (a) ω and (b) γ of the $A_{1g}(O_a)$ mode in Tl-2201 (black symbols), Tl-2212 (red symbols), and Tl-2223 (blue symbols). The vertical dashed line corresponds to T_c.

Tl-2223 from 150 K to T_c. The γ value has 1 cm^{-1} narrowing from 300–200 K in Tl-2212 and Tl-2223, and becomes constant at the low temperature. The γ value nearly does not change in Tl-2201 if there is any variation for the data at lower temperatures ($<T_c$). The phonon softening was also reported on Tl-based compounds in the early study [46]. The $A_{1g}(O_{Tl-O})$ modes show a slight softening near T_c in Tl-2201, Tl-2212, and Tl-2223. Comparing to the other cuprate superconductors such as $Bi_2Sr_2CaCu_2O_{8+\delta}$ [49], the A_{1g} mode at 650 cm^{-1} showed an overall phonon hardening from 300–10 K.

IV. DISCUSSION

A. Superconductivity-induced self-energy effect

In the conventional superconductor, the effect of superconductivity on the phonon modes is usually weak. The evolution of the phonon frequencies in the microscopic picture is determined by some electronic excitations. Only the electronic states near the Fermi surface are changed as the sample enters

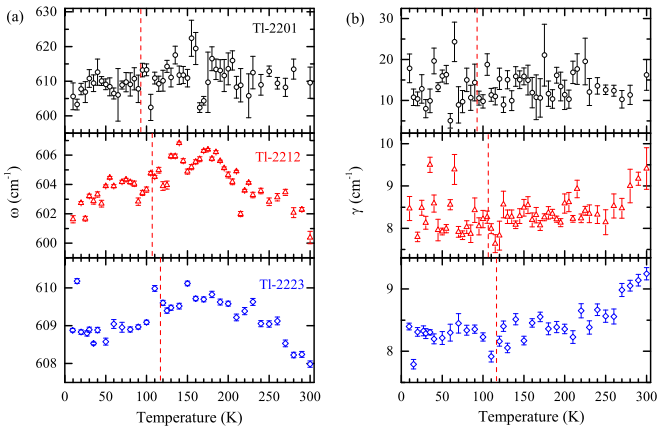

FIG. 6. Temperature dependence of the (a) ω and (b) γ of the $A_{1g}(O_{Tl-O})$ mode in Tl-2201 (black symbols), Tl-2212 (red symbols), and Tl-2223 (blue symbols). The vertical dashed line corresponds to T_c.

TABLE II. Summary of the superconducting gap size (2Δ), superconducting fluctuation temperature (T_{SF}), and pseudogap onset temperature (T^{PG}) of Tl-based family from the works in the literature.

Sample	Tl-2201	Tl-2212	Tl-2223
T_c(K)	85–91	91–112	114–120
2Δ(cm^{-1})	306–403 [82,83]	322–451 [84–86]	371–564 [87–89]
T_{SF}(K)	97.5 [96,97]	120–150 [98–100]	135–150 [101]
T^{PG}(K)	115–125 [41]	130–170 [42]	140–160 [43]

the superconducting state. The self-energy effect [78] is due to the redistribution of the electronic density near the Fermi surface induced by the interaction between the phonon states and electrons. The effects are so small in cuprates that the phonons must be carefully measured with high accuracy and resolution [48,49,51]. According to the self-energy model [78,79], the energy gap (2Δ) opens due to superconductivity, producing the change in the self-energy $\Delta\Sigma = \Delta\omega + i\Delta\gamma$. The real part ($\Delta\omega$) represents the shift of the frequency, and the imaginary part ($\Delta\gamma$) is the variation in the linewidth. From the strong-coupling theory, the change of the phonon self-energy is affected by the ratio of $\omega/2\Delta$, and the corresponding results at different ratios are predicted. When $\omega < 2\Delta$, the phonon will be softened after entering the superconducting state, and the linewidth is expected to exhibit broadening. When ω is close to the position of 2Δ, the frequency will show obvious softening near T_c, and the linewidth can increase significantly. When $\omega > 2\Delta$, the frequency will show a monotonically increasing (hardening) trend, while the linewidth will continue to decrease.

It is necessary to determine the location of the superconducting gap before the phonon analysis. The bulk probes (Raman scattering, IR spectroscopy) [80,81] and the surface probes (electron tunneling spectroscopy, point-contact spectroscopy, break-junction tunneling spectroscopy, Andreev reflection spectroscopy) [82–89] are the two major families of methods used to obtain 2Δ in the Tl-based materials. Tl-based compounds measured here are nearly optimally doped. Therefore, the 2Δ values should be used from the optimally doped Tl-based samples. Table II summarizes the early results from the tunneling spectroscopy [82–89]. 2Δ position increases with the increase of T_c. For single-layer Tl-2201, T_c is between 85 and 91 K, Δ value obtained by point contact spectroscopy is about 19–25 meV, corresponding to 2Δ of about 306–403 cm^{-1}. The bilayer Tl-2212 has the Δ of about 20–28 meV, and the corresponding 2Δ is at 322–451 cm^{-1} when T_c is in the range of 91–112 K. For trilayer Tl-2223, the critical temperature is about 114–120 K, and the tunneling spectra give the Δ value at 23–35 meV, yielding 2Δ in the range of 371–564 cm^{-1}.

The position of the A_{1g}(Tl) mode for the studied Tl-2201, Tl-2212, and Tl-2223 is at 162, 133, and 132 cm^{-1}, respectively. Comparing to 2Δ, which is generally higher than 300 cm^{-1}, the ratio of $\omega/2\Delta$ is less than 0.5. According to the self-energy model [78], the phonon mode in this range ($\omega/2\Delta = 0.2$–0.5) will soften after entering the superconducting state, and the linewidth is expected to exhibit a little broadening. Referring to the analysis in Fig. 4, the self-energy model does not match the evolution of the observed

behaviors of this low-frequency mode. Single-layer Tl-2201 and bilayer Tl-2212 exhibit phonon softening at T_c. However, their linewidths stay unchanged at low temperatures. For trilayer Tl-2223, the frequency is slightly hardened, and the corresponding linewidth remains nearly constant below T_c. Clearly, this A_{1g}(Tl) mode does not obey the expected self-energy effect.

The $A_{1g}(O_a)$ mode in Tl-2201, Tl-2212, and Tl-2223 is located at 491, 494, and 501 cm^{-1}, respectively. Such values of ω are close to 2Δ. It is thus expected to have a stronger self-energy effect. The ratio $\omega/2\Delta$ is about 1.2–1.6 in Tl-2201, thus the frequency should show a significant hardening near T_c according to self-energy model [78], accompanied by a significant broadening in the linewidth. From the results on Tl-2201 as shown in Fig. 5, the frequency shows a smooth phonon softening at low temperatures, and the corresponding linewidth remains stable below T_c. For bilayer Tl-2212, $\omega/2\Delta$ is 1.1–1.5. The frequency is expected to decrease, while the linewidth will show an obvious narrowing. The experiments give a decreasing frequency after entering the superconducting state and a nearly constant linewidth below T_c. Finally, the $\omega/2\Delta$ of the trilayer sample is about 0.9–1.3. It is expected to have a significant softening in the frequency, accompanied by a broadening of the linewidth. From the temperature dependence of the Raman spectra (Fig. 5), the frequency of the trilayer sample shows hardening near T_c, while the linewidth shows a slight narrowing. Therefore, there is a big difference between the theoretical expectations from the self-energy model and experimental results.

The $A_{1g}(O_{Tl-O})$ mode of Tl-2201, Tl-2212, and Tl-2223 is located at 603, 602, and 608 cm^{-1}, respectively. These values for the high-frequency modes are much higher than the corresponding 2Δ positions. For single-layer Tl-2201, $\omega/2\Delta$ is about 1.5–1.97, the frequency is expected to show a monotonic increase on cooling, and the linewidth decreases. In Fig. 6, the frequency of Tl-2201 shows a slight softening at low temperatures, and the linewidth remains unchanged. For bilayer Tl-2212, $\omega/2\Delta$ is about 1.3–1.9, the frequency and linewidth tend to exhibit behaviors similar to those observed in the single-layer compound. However, the frequency of the bilayer sample shows a softening behavior in the superconducting state, and the linewidth in general remains unchanged. Since $\omega/2\Delta$ is about 1.1–1.6 for Tl-2223, the frequency is expected to decrease, while the linewidth will show an obvious narrowing. However, the results in Fig. 6 reveal that the trilayer sample still exhibits a smooth softening through T_c, and the corresponding linewidth does not change significantly but rather keeping a nearly constant. Hence, the behaviors of this high-frequency mode do not follow the self-energy model as well.

All the selected modes in the studied Tl-based compounds do not follow the expected self-energy effect below T_c. The phonon anomalies with the softening frequency upon decreasing temperature are observed for the A_{1g}(Tl), $A_{1g}(O_a)$, and $A_{1g}(O_{Tl-O})$ mode at around 150 K in all these Tl-based materials. The apical oxygen mode $A_{1g}(O_a)$ exhibits a more pronounced universal phonon softening below 150 K. The origin of this kind of phonon behavior might have important implications for the understanding of superconductivity in cuprates.

B. Origin of the phonon softening

The superconducting fluctuation may extend to the normal state above T_c in cuprate superconductors [90,91]. To prove the superconducting fluctuations above T_c, one of the effective ways is to measure the Nernst effect [5]. This method has been used to address the possible existence of vortex excitations in the pseudogap region of the cuprate superconductors. The theoretical work [92] based on the vortex liquid state suggests that the Nernst signal should exhibit an increase in the low-field region, and then it drops down when the magnetic field is close to a certain ratio to the upper critical field.

To find out the relationship between the phonon softening and the superconducting fluctuations, the onset temperature (T_{SF}) for such fluctuations should be located. Some evidence for fluctuating superconductivity has been inferred from the measurements of the Nernst effect [5], in-plane angle-dependent resistance [93], time-domain optical conductivity [94], and specific heat [90,95], etc. Table II gives the results of the measurements from various techniques [96–101]. For single-layer sample Tl-2201, T_c was measured to be 87–90 K, and the corresponding T_{SF} is about 97.5 K. For bilayer Tl-2212, T_c of the prepared sample is 105–106 K, T_{SF} is near 120 K. For trilayer Tl-2223, T_c was measured to be 119 K and T_{SF} is about 135 K.

The universal phonon softening is observed at about 150 K from the temperature dependence of the Raman spectra. For single-layer Tl-2201, T_{SF} is much lower than this temperature. While for bilayer Tl-2212 and trilayer Tl-2223, T_{SF} is close to the initial softening temperature. Thus, phonon softening is not directly related to superconducting fluctuations for the single-layer compound. However, such a possibility can not be ruled out for the bilayer and trilayer samples.

The charge density wave (CDW) state appears in the normal state and was widely reported in cuprate superconductors [15,102–104]. Its origin is rooted in the instability of an one-dimensional system as described by Peierls. The extension of this concept to other systems has led to the concept of the Fermi surface nesting, which dictates the wave vector of the CDW and the corresponding lattice distortion [105].

To detect the charge order in cuprate superconductors, resonant x-ray scattering (RXS) [15,16,106], scanning-tunneling microscopy (STM) [16,103,106], and ARPES [106] were extensively carried out. However, atomic resolution STM images show that almost all the surface has a near-trigonal structure in optimally doped Tl-2212 and Tl-2223 [107]. It is different from a checkerboard pattern in bilayer Bi-2212 single crystal [16,103]. For single-layer Tl-2201, the CDW state was detected even in the overdoped region (T_c = 30 K). It was explained by a Fermi surface reconstruction, which is contrary to the case of under- and optimally doped cuprates [108,109]. Thus, the direct evidence for measuring the CDW state in optimally doped Tl-based materials is still lacking.

Therefore, we have to focus on the pseudogap above T_c. It is a consequence of two basic properties of high-T_c superconductors: The d-wave nature of the superconducting gap function varying as the cosine function around the Fermi surface, and the persistence of this gap into the normal state [1].

ARPES [4,7,8], tunneling spectroscopy [110,111], nuclear magnetic resonance (NMR) [41–43], and electrical transport [112,113] can be directly used to detect the existence of the pseudogap in cuprates. Table II gives the onset temperature of the pseudogap (T^{PG}) in the optimally doped Tl-based samples from NMR measurements [41–43]. The T_c value of the single-layer Tl-2201 is 85 K, while the T^{PG} value was determined at about 115–125 K [41]. For bilayer Tl-2212, T_c was measured to be 112 K, the corresponding T^{PG} was found around 130–170 K [42]. For trilayer Tl-2223, T_c of the as-grown sample is about 115 K, and the value of T^{PG} is about 140–160 K [43].

For single-layer Tl-2201, T^{PG} is very close to the observed 150 K of the phonon softening temperature. Meanwhile, the temperature range of the pseudogap values covers the softening regime for Tl-2212 and Tl-2223. From this unexpected coincidence, it is not difficult to relate the observed softening to the interaction between the corresponding phonons and pseudogap. According to the band-structure calculations, pseudogaps are theoretically associated with the strong spin-phonon coupling [114]. In this model, the Coulomb potential from the phonon modes and the spin-polarized part of the potential from the spin waves contribute to the opening of a partial gap at the Fermi energy. The phonon softening is used to estimate the obtained kinetic energy of the gap. This softening will be weak when the temperature is close to T_c. Figures 4–6 show that the phonon softening does emerge in Tl-based family at a high temperature above T_c rather than entering the superconducting state. The theory also predicts that the atomic displacement will enhance the spin-phonon effect and the pseudogap value. The misalignment of atoms between the atomic layers in a normal state was indeed observed for the Tl-based samples [115–117]. These vibrational displacements suggest a dramatic phonon softening far above T_c. Besides, the specific heat measurements show that T_{SF} occurs between T_c and T^{PG} [90,95] in the underdoped and optimally doped cuprate superconductors. This is also consistent with the present results. That is, the phonon softening temperature is generally higher than T_{SF}.

The obvious softening behaviors observed for Tl-based family are nicely consistent with the theoretical model within the strong spin-phonon coupling [114]. It is thus indicated that these universal softening trends are related to the pseudogap state from the analysis and comparisons of the existing experimental data. It is interesting to note that the similar phonon anomalies below and above T^{PG} were also reported previously for $YBa_2Cu_3O_{7-\delta}$ by analyzing the in-plane optical conductivity data [118]. Such behaviors in the optical conductivity spectra were suggested to be associated with pair formation at T^{PG} and the Bose-Einstein condensation of the preformed pairs. Within this framework, the significant softening of the $A_{1g}(O_a)$ mode observed in Tl-2201, Tl-2212, and Tl-2223 highlight the important role of this phonon branch played for the pairing and the coupling to the electronic charge excitations.

C. Possible phonon effect on the pseudogap

The universal phonon softening far above T_c may provide evidence of the tight relationship between the superconductivity and the pseudogap. According to the promising theory for high-T_c superconductivity [19], pseudogap is a precursor pairing and originates only from the spin-charge coupling. In this case, there is only a superconducting pairing in the normal state and no phonon contribution in the pseudogap state is expected. ω and γ are likely to exhibit the corresponding self-energy effect after entering the superconducting state. This picture seemingly gets the experimental supports for the feature of the magnetic order for the pseudogap [11–13]. However, the observed evolution of the phonon mode with temperature does not follow such the theoretical predictions. Along with the reported huge isotope effect on the opening temperature of the pseudogap [26–28], the present results strongly indicate that the large lattice effect should be included in the understanding of the pseudogap phenomenon in cuprates.

The anomalous softening behavior detected for the Tl-based family indicates the non-negligible lattice effect on the phonon modes. It seems that the opening of the pseudogap at least shares a part of the self-energy effect. As a result, the reduction of total self-energy and a weak self-energy effect when entering the superconducting state may follow [68]. From our results, the decreasing frequency and unchangeable linewidth show a drastic self-energy loss at the temperature above T_c. Therefore, all the selected phonon modes, even the $A_{1g}(O_a)$ mode, which is closest to 2Δ, do not follow the expected behaviors in the superconducting state. In addition, the effect of the pseudogap is so powerful that it masks the superconductivity-induced phonon anomalies. It is why all the detected phonon modes continue to decrease during cooling when passing through the superconducting transition. Considering the evidence for the magnetic signature of the pseudogap [11–13,21–24], the present results might suggest the magnon-phonon coupling in the pseudogap state [119].

V. CONCLUSIONS

In conclusion, we have used Raman scattering spectroscopy to investigate the vibrational properties of high-quality $Tl_2Ba_2Ca_{n-1}Cu_nO_{2n+4+\delta}$ ($n = 1, 2, 3$) single crystals in the normal and superconducting state. The universal phonon softening at temperature near 150 K above the superconducting transition of each phonon mode has been generally observed. These phonon modes do not follow the expected self-energy effect. Instead, the feature can be related to the formation of the pseudogap state. The starting temperature for the phonon softening was found to be the opening temperature for the pseudogap. The results suggest the non-negligible lattice effect in the pseudogap state.

ACKNOWLEDGMENTS

The work at HPSTAR was supported by the National Key R&D Program of China (Grant No. 2018YFA0305900). V.V.S. acknowledges the financial support from Shanghai Science and Technology Committee, China (No. 22JC1410300) and Shanghai Key Laboratory of Material Frontiers Research in Extreme Environments, China (No. 22dz2260800).

[1] T. Timusk and B. Statt, The pseudogap in high-temperature superconductors: An experimental survey, Rep. Prog. Phys. **62**, 61 (1999).

[2] M. R. Norman, D. Pines, and C. Kallin, The pseudogap: Friend or foe of high T_c? Adv. Phys. **54**, 715 (2005).

[3] H. Ding, T. Yokoya, J. C. Campuzano, T. Takahashi, M. Randeria, M. R. Norman, T. Mochiku, K. Kadowaki, and J. Giapintzakis, Spectroscopic evidence for a pseudogap in the normal state of underdoped high-T_c superconductors, Nature (London) **382**, 51 (1996).

[4] J. M. Harris, P. J. White, Z. X. Shen, H. Ikeda, R. Yoshizaki, H. Eisaki, S. Uchida, W. D. Si, J. W. Xiong, Z. X. Zhao, and D. S. Dessau, Measurement of an Anisotropic Energy Gap in Single Plane $Bi_2Sr_{2-x}La_xCuO_{6+\delta}$, Phys. Rev. Lett. **79**, 143 (1997).

[5] Z. A. Xu, N. P. Ong, Y. Wang, T. Kakeshita, and S. Uchida, Vortex-like excitations and the onset of superconducting phase fluctuation in underdoped $La_{2-x}Sr_xCuO_4$, Nature (London) **406**, 486 (2000).

[6] J. Q. Meng, W. T. Zhang, G. D. Liu, L. Zhao, H. Y. Liu, X. W. Jia, W. Lu, X. L. Dong, G. L. Wang, H. B. Zhang, Y. Zhou, Y. Zhu, X. Y. Wang, Z. X. Zhao, Z. Xu, C. T. Chen, and X. J. Zhou, Monotonic d-wave superconducting gap of the optimally doped $Bi_2Sr_{1.6}La_{0.4}CuO_6$ superconductor by laser-based angle-resolved photoemission spectroscopy, Phys. Rev. B **79**, 024514 (2009).

[7] A. Kanigel, U. Chatterjee, M. Randeria, M. R. Norman, S. Souma, M. Shi, Z. Z. Li, H. Raffy, and J. C. Campuzano, Protected Nodes and the Collapse of Fermi Arcs in high-T_c Cuprate Superconductors, Phys. Rev. Lett. **99**, 157001 (2007).

[8] H. Ding, M. R. Norman, T. Yokoya, T. Takeuchi, M. Randeria, J. C. Campuzano, T. Takahashi, T. Mochiku, and K. Kadowaki, Evolution of the Fermi Surface with Carrier Concentration in $Bi_2Sr_2CaCu_2O_{8+\delta}$, Phys. Rev. Lett. **78**, 2628 (1997).

[9] M. Hashimoto, R. H. He, K. Tanaka, J. P. Testaud, W. Meevasana, R. G. Moore, D. H. Lu, H. Yao, Y. Yoshida, H. Eisaki, T. P. Devereaux, Z. Hussain, and Z. X. Shen, Particle hole symmetry breaking in the pseudogap state of Bi2201, Nature Phys. **6**, 414 (2010).

[10] H. B. Yang, J. D. Rameau, P. D. Johnson, T. Valla, A. Tsvelik, and G. D. Gu, Emergence of preformed Cooper pairs from the doped Mott insulating state in $Bi_2Sr_2CaCu_2O_{8+\delta}$, Nature (London) **456**, 77 (2008).

[11] Z. C. Wang, K. Pei, L. T. Yang, C. D. Yang, G. Y. Chen, X. B. Zhao, C. Wang, Z. W. Liu, Y. Li, R. C. Che, and J. Zhu, Topological spin textture in the pseudogap phase of a high-T_c superconductor, Nature (London) **615**, 405 (2023).

[12] B. Fauqué, Y. Sidis, V. Hinkov, S. Pailhès, C. T. Lin, X. Chaud, and P. Bourges, Magnetic Order in the Pseudogap Phase of High-T_c Superconductors, Phys. Rev. Lett. **96**, 197001 (2006).

[13] Y. Li, V. Balédent, N. Barišić, Y. Cho, B. Fauqué, Y. Sidis, G. Yu, X. Zhao, P. Bourges, and M. Greven, Unusual magnetic order in the pseudogap region of the superconductor $HgBa_2CuO_{4+\delta}$, Nature (London) **455**, 372 (2008).

[14] M. Hashimoto, E. A. Nowadnick, R. H. He, I. M. Vishik, B. Moritz, Y. He, K. Tanaka, R. G. Moore, D. Lu, Y. Yoshida, M. Ishikado, T. Sasagawa, K. Fujita, S. Ishida, S. Uchida, H. Eisaki, Z. Hussain, T. P. Devereaux, and Z. X. Shen, Direct spectroscopic evidence for phase competition between the pseudogap and superconductivity in $Bi_2Sr_2CaCu_2O_{8+\delta}$, Nature Mater. **14**, 37 (2015).

[15] G. Ghiringhelli, M. L. Tacon, M. Minola, S. Blanco-canosa, C. Mazzoli, N. B. Brookes, G. M. D. Luca, A. Frano, D. G. Hawthorn, F. He, T. Loew, M. M. Sala, D. C. Peets, M. Salluzzo, E. Schierle, R. Sutarto, G. A. Aawatzky, E. Weschke, B. Keimer, and L. Braicovich, Long-range incommensurate charge fluctuations in (Y, Nd)$Ba_2Cu_3O_{6+x}$, Science **337**, 821 (2012).

[16] E. H. da Silva Neto, P. Aynajian, A. Frano, R. Comin, E. Schierle, E. Weschke, A. Gyenis, J. S. Wen, J. Schneeloch, Z. J. Xu, S. Ono, G. D. Gu, M. L. Tacon, and A. Yazdani, Ubiquitous interplay between charge ordering and high-temperature superconductivity in cuprates, Science **343**, 393 (2014).

[17] J. Chang, E. Blackburn, A. T. Holmes, N. B. Christensen, J. Larsen, J. Mesot, R. X. Liang, D. A. Bonn, W. N. Hardy, A. Watenphul, M. V. Zimmermann, E. M. Forgan, and S. M. Hayden, Direct observation of competition between superconductivity and charge density wave order in $YBa_2Cu_3O_{6.67}$, Nature Phys. **8**, 871 (2012).

[18] A. Kaminski, S. Rosenkranz, H. M. Fretwell, J. C. Campuzano, Z. Li, H. Raffy, W. G. Cullen, H. You, C. G. Olson, C. M. Varma, and H. Höchst, Spontaneous breaking of time-reversal symmetry in the pseudogap state of a high-T_c superconductor, Nature (London) **416**, 610 (2002).

[19] P. W. Anderson, P. A. Lee, M. Randeria, T. M. Rice, N. Trivedi, and F. C. Zhang, The physics behind high-temperature superconducting cuprates: The plain vanilla version of RVB, J. Phys.: Condens. Matter **16**, R755 (2004).

[20] A. A. Kordyuk, Pseudogap from ARPES experiment: Three gaps in cuprates and topological superconductivity, Low Temp. Phys. **41**, 319 (2015).

[21] S. Sugai and T. Hosokawa, Relation between the Superconducting Gap Energy and the Two-Magnon Raman Peak Energy in $Bi_2Sr_2Ca_{1-x}Y_xCu_2O_{8+\delta}$, Phys. Rev. Lett. **85**, 1112 (2000).

[22] S. Sugai, H. Suzuki, Y. Takayanagi, T. Hosokawa, and N. Hayamizu, Carrier-density-dependent momentum shift of the coherent peak and the LO phonon mode in p-type high-T_c superconductors, Phys. Rev. B **68**, 184504 (2003).

[23] Y. Li, M. Le Tacon, M. Bakr, D. Terrade, D. Manske, R. Hackl, L. Ji, M. K. Chan, N. Barišić, X. Zhao, M. Greven, and B. Keimer, Feedback Effect on High-Energy Magnetic Fluctuations in the Model High-Temperature Superconductor $HgBa_2CuO_{4+\delta}$ Observed by Electronic Raman Scattering, Phys. Rev. Lett. **108**, 227003 (2012).

[24] B. Mansart, J. Lorenzana, A. Mann, A. Odeh, M. Scarongella, M. Chergui, and F. Carbone, Coupling of a high-energy excitation to superconducting quasiparticles in a cuprate from coherent charge fluctuation spectroscopy, Proc. Natl. Acad. Sci. USA **110**, 4539 (2013).

[25] N. Lin, E. Gull, and A. J. Millis, Two-Particle Response in Cluster Dynamical Mean-Field Theory: Formalism and Application to the Raman Response of High-Temperature Superconductors, Phys. Rev. Lett. **109**, 106401 (2012).

[26] M. Bendele, F. V. Rohr, Z. Guguchia, E. Pomjakushina, K. Conder, A. Bianconi, A. Simon, A. Bussmann-Holder, and H. Keller, Evidence for strong lattice effects as revealed from huge unconventional oxygen isotope effects on the pseudogap temperature in $La_{2-x}Sr_xCuO_4$, Phys. Rev. B **95**, 014514 (2017).

[27] D. Rubio Temprano, J. Mesot, S. Janssen, K. Conder, A. Furrer, H. Mutka, and K. A. Müller, Large Isotope Effect on the Pseudogap in the High-Temperature Superconductor $HoBa_2Cu_4O_8$, Phys. Rev. Lett. **84**, 1990 (2000).

[28] A. Lanzara, G. M. Zhao, N. L. Saini, A. Bianconi, K. Conder, H. Keller and K. A. Müller, Oxygen-isotope shift of the charge-stripe ordering temperature in $La_{2-x}Sr_xCuO_4$ from x-ray absorption spectroscopy, J. Phys.: Condens. Matter **11**, L541 (1999).

[29] Z. Z. Sheng, A. M. Hermann, A. E. Ali, C. Almasan, J. Estrada, T. Datta, and R. J. Matson, Superconductivity at 90 K in the Tl-Ba-Cu-O System, Phys. Rev. Lett. **60**, 937 (1988).

[30] R. M. Hazen, L. W. Finger, R. J. Angel, C. T. Prewitt, N. L. Ross, C. G. Hadidiacos, P. J. Heaney, D. R. Veblen, Z. Z. Sheng, A. El Ali, and A. M. Hermann, 100-K Superconducting Phases in the Tl-Ca-Ba-Cu-O System, Phys. Rev. Lett. **60**, 1657 (1988).

[31] X. J. Chen, B. Liang, C. Ulrich, C. T. Lin, V. V. Struzhkin, Z. Wu, R. J. Hemley, H. K. Mao, and H. Q. Lin, Oxygen isotope effect in $Bi_2Sr_2Ca_{n-1}Cu_nO_{2n+4+\delta}$ ($n = 1, 2, 3$) single crystals, Phys. Rev. B **76**, 140502(R) (2007).

[32] X. J. Chen, V. V. Struzhkin, Z. Wu, H. Q. Lin, R. J. Hemley, and H. K. Mao, Unified picture of the oxygen isotope effect in cuprate superconductors, Proc. Natl. Acad. Sci. USA **104**, 3732 (2007).

[33] X. J. Chen, V. V. Struzhkin, Z. Wu, R. J. Hemley, H. K. Mao, and H. Q. Lin, Phonon-mediated superconducting transitions in layered cuprate superconductors, Phys. Rev. B **75**, 134504 (2007).

[34] A. A. Tsvetkov, D. Dulić, D. van der Marel, A. Damascelli, G. A. Kaljushnaia, J. I. Gorina, N. N. Senturina, N. N. Kolesnikov, Z. F. Ren, J. H. Wang, A. A. Menovsky, and T. T. M. Palstra, Systematics of *c*-axis phonons in the thallium- and bismuth-based cuprate superconductors, Phys. Rev. B **60**, 13196 (1999).

[35] R. Liu, C. Thomsen, W. Kress, M. Cardona, B. Gegenheimer, F. W. de Wette, J. Prade, A. D. Kulkarni, and U. Schröder, Frequencies, eigenvectors, and single-crystal selection rules of $k = 0$ phonons in $YBa_2Cu_3O_{7-\delta}$: Theory and experiment, Phys. Rev. B **37**, 7971 (1988).

[36] N. N. Kovaleva, A. V. Boris, T. Holden, C. Ulrich, B. Liang, C. T. Lin, B. Keimer, C. Bernhard, J. L. Tallon, D. Munzar, and A. M. Stoneham, *c*-axis lattice dynamics in Bi-based cuprate superconductors, Phys. Rev. B **69**, 054511 (2004).

[37] D. E. Cox, C. C. Torardi, M. A. Subrumanian, J. Gopalakrishnan, and A. W. Sleight, Structure refinements of superconducting $Tl_2Ba_2CaCu_2O_8$ and $Tl_2Ba_2Ca_2Cu_3O_{10}$ from neutron diffraction data, Phys. Rev. B **38**, 6624 (1988).

[38] H. Yamauchi and T. Kaneko, Higher temperaturization of Tl-2223 superconductors, Phase Transitions **41**, 21 (1993).

[39] L. V. Gasparov, V. D. Kulakovskii, O. V. Misochko, A. A. Polyanskii, and V. B. Timofeev, Raman study of Tl-based superconducting single crystals: Phonons assignment and temperature dependence, Physica C: Supercond. **160**, 147 (1989).

[40] T. Zetterer, M. Franz, J. Schiitzmann, W. Ose, H. H. Otto, and K. F. Renk, Anomalous behavior of phonons in superconducting $Tl_2Ba_2Ca_2Cu_3O_{10}$ detected by far-infrared spectroscopy, Phys. Rev. B **41**, 9499 (1990).

[41] S. Kambe, H. Yasuoka, A. Hayashi, and Y. Ueda, NMR study of the spin dynamics in $Tl_2Ba_2CuO_y$ ($T_c = 85$ K), Phys. Rev. B **47**, 2825 (1993).

[42] A. Gerashenko, Y. Piskunov, K. Mikhalev, A. Ananyev, K. Okulova, S. Verkhovskii, A. Yakubovskii, L. Shustov, and A. Trokiner, The ^{63}Cu and ^{17}O NMR studies of spin susceptibility in differently doped $Tl_2Ba_2CaCu_2O_{8-\delta}$ compounds, Physica C: Supercond. **328**, 163 (1999).

[43] G. Q. Zheng, Y. Kitaoka, K. Asayama, K. Hamada, H. Yamauchi, and S. Tanaka, NMR study of local hole distribution, spin fluctuation and superconductivity in $Tl_2Ba_2Ca_2Cu_3O_{10}$, Physica C: Supercond. **260**, 197 (1996).

[44] A. Mukherjee, D. Z. Liu, A. T. Boothroyd, L. Y. Su, C. R. M. Grovenor, and M. J. Goringe, Raman-active phonon softening in a Tl-Ba-Ca-Cu-O superconducting thin film, Solid State Commun. **93**, 747 (1995).

[45] J. Chrzanowski, N. Fortier, A. Cragg, S. Burany, B. Heinrich, and J. C. Irwin, Temperature dependence of the Raman spectra of $Tl_2Ba_2CaCu_2O_8$, Physica C: Supercond. **185-189**, 649 (1991).

[46] K. Matsuishi, Y. Q. Yang, Y. Y. Sun, J. G. Lin, P. H. Hor, M. Gorman, and C. W. Chu, Systematic Raman study on TI-based superconductors with T_c-variation due to oxygen deficiency, Proc. SPIE **1336**, 93 (1990).

[47] C. Thomsen, M. Cardona, B. Gegenheimer, R. Liu, and A. Simon, Untwinned single crystals of $YBa_2Cu_3O_{7-\delta}$: An optical investigation of the *ab* anisotropy, Phys. Rev. B **37**, 9860 (1988).

[48] G. Burns, G. V. Chandrashekhar, F. H. Dacol, and P. Strobel, Temperature dependence of the Raman spectra for $Bi_2Sr_2CaCu_2O_8$, Phys. Rev. B **39**, 775(R) (1989).

[49] M. Boekholt, A. Erle, P. C. Splittgerber-Hiinnekes, and G. Güntherodt, Phonon Raman spectroscopy of superconducting $Bi_2Sr_2CaCu_2O_{8+\delta}$ single crystals, Solid State Commun. **74**, 1107 (1990).

[50] I. Loa, J. Hoffmann, A. P. Litvinchuk, and C. Thomsen, Superstructure of $Bi_2Sr_2CaCu_2O_8$ superconductors: A Raman-scattering study, Proc. SPIE **693**, 248 (1996).

[51] X. J. Zhou, M. Cardona, D. Colson, and V. Viallet, Plane oxygen vibrations and their temperature dependence in $HgBa_2Ca_2Cu_3O_{8+\delta}$ single crystals, Phys. Rev. B **55**, 12770 (1997).

[52] M. F. Limonov, A. I. Rykov, S. Tajima, and A. Yamanaka, Superconductivity-induced effects on phononic and electronic Raman scattering in twin-free $YBa_2Cu_3O_{7-x}$ single crystals, Phys. Rev. B **61**, 12412 (2000).

[53] K. C. Hewitt, X. K. Chen, C. Roch, J. Chrzanowski, J. C. Irwin, E. H. Altendorf, R. Liang, D. Bonn, and W. N. Hardy, Hole concentration and phonon renormalization of the 340 cm^{-1} B_{1g} mode in 2% Ca-doped $YBa_2Cu_3O_y$ ($6.76 \leqslant y \leqslant 7.00$), Phys. Rev. B **69**, 064514 (2004).

[54] X. J. Chen, V. V. Struzhkin, Y. Yu, A. F. Goncharov, C. T. Lin, H. K. Mao, and R. J. Hemley, Enhancement of superconductivity by pressure-driven competition in electronic order, Nature (London) **466**, 950 (2010).

[55] B. Friedl, C. Thomsen, and M. Cardona, Determination of the Superconducting Gap in $RBa_2Cu_3O_{7-\delta}$, Phys. Rev. Lett. **65**, 915 (1990).

[56] A. Yamanaka, H. Takato, F. Minami, K. Inoue, and S. Takekawa, Temperature dependence of electronic Raman-

scattering spectra in superconducting $Bi_2Sr_2CaCu_2O_{8+\delta}$ single crystals, Phys. Rev. B **46**, 516 (1992).

[57] R. Nemetschek, O. V. Misochko, B. Stadlober, and R. Hackl, Inelastic light scattering from electronic and phononic excitations in normal and superconducting $Tl_2Ba_2CuO_6$ single crystals, Phys. Rev. B **47**, 3450 (1993).

[58] X. K. Chen, J. C. Irwin, H. J. Trodahl, T. Kimura, and K. Kishio, Investigations of the Superconducting Gap in $La_{2-x}Sr_xCuO_4$ by Raman Spectroscopy, Phys. Rev. Lett. **73**, 3290 (1994).

[59] C. Kendziora, R. J. Kelley, and M. Onellion, Superconducting Gap Anisotropy vs Doping Level in high-T_c Cuprates, Phys. Rev. Lett. **77**, 727 (1996).

[60] M. Rübhausen, P. Guptasarma, D. G. Hinks, and M. V. Klein, Spin and charge excitations in optimally doped $Bi_2Sr_2CaCu_2O_{8-\delta}$, Phys. Rev. B **58**, 3462 (1998).

[61] K. C. Hewitt and J. C. Irwin, Doping dependence of the superconducting gap in $Bi_2Sr_2CaCu_2O_{8+\delta}$, Phys. Rev. B **66**, 054516 (2002).

[62] T. Masui, M. Limonov, H. Uchiyama, S. Lee, S. Tajima, Raman study of carrier-overdoping effects on the gap in high-T_c superconducting cuprates, Phys. Rev. B **68**, 060506 (2003).

[63] M. Le Tacon, A. Sacuto, A. Georges, G. Kotliar, Y. Gallais, D. Colson, and A. Forget, Two energy scales and two distinct quasiparticle dynamics in the superconducting state of underdoped cuprates, Nature Phys. **2**, 537 (2006).

[64] S. Blanc, Y. Gallais, A. Sacuto, M. Cazayous, M. A. Méasson, G. D. Gu, J. S. Wen, and Z. J. Xu, Quantitative Raman measurement of the evolution of the Cooper-pair density with doping in $Bi_2Sr_2CaCu_2O_{8+\delta}$ superconductors, Phys. Rev. B **80**, 140502(R) (2009).

[65] B. Loret, N. Auvray, Y. Gallais, M. Cazayous, A. Forget, D. Colson, M. H. Julien, I. Paul, M. Civelli, and A. Sacuto, Intimate link between charge density wave, pseudogap and superconducting energy scales in cuprates, Nature Phys. **15**, 771 (2019).

[66] B. Loret, N. Auvray, G. D. Gu, A. Forget, D. Colson, M. Cazayous, Y. Gallais, I. Paul, M. Civelli, and A. Sacuto, Universal relationship between the energy scales of the pseudogap phase, the superconducting state, and the charge-density-wave order in copper oxide superconductors, Phys. Rev. B **101**, 214520 (2020).

[67] G. Blumberg, M. Kang, M. V. Klein, K. Kadowaki, and C. Kendziora, Evolution of magnetic and superconducting fluctuations with doping of high-T_c superconductors, Science **278**, 1427 (1997).

[68] M. F. Limonov, S. Tajima, and A. Yamanaka, Phononic and electronic Raman spectroscopy of the pseudogap state in underdoped $YBa_2Cu_3O_{7-\delta}$, Phys. Rev. B **62**, 11859 (2000).

[69] T. Masui, T. Hiramachi, K. Nagasao, and S. Tajima, Electronic crossover in the overdoped high-temperature (Y, Ca)$Ba_2Cu_3O_y$ superconductor by Raman scattering, Phys. Rev. B **79**, 014511 (2009).

[70] B. Loret, Y. Gallais, M. Cazayous, R. D. Zhong, J. Schneeloch, G. D. Gu, A. Fedorov, T. K. Kim, S. V. Borisenko, and A. Sacuto, Raman and ARPES combined study on the connection between the existence of the pseudogap and the topology of the Fermi surface in $Bi_2Sr_2Ca\ Cu_2O_{8+\delta}$, Phys. Rev. B **97**, 174521 (2018).

[71] Y. C. Ma and N. L. Wang, Crystal growth and in-plane optical properties of $Tl_2Ba_2Ca_{n-1}Cu_nO_x (n = 1, 2, 3)$ superconductors, Phys. Rev. B **72**, 104518 (2005).

[72] J. B. Zhang, V. V. Struzhkin, W. G. Yang, H. K. Mao, H. Q. Lin, Y. C. Ma, N. L. Wang, and X. J. Chen, Pressure tuning of superconductivity independent of disorder in $Tl_2Ba_2CaCu_2O_{8+\delta}$, J. Phys.: Condens. Matter **27**, 445701 (2015).

[73] A. D. Kulkarni, F. W. de Wette, J. Prade, U. Schröder, and W. Kress, Phonon spectra and lattice specific heats of the thallium-based high-temperature superconductors, Phys. Rev. B **43**, 5451 (1991).

[74] A. D. Kulkarni, F. W. de Wette, J. Prade, U. Schröder, and W. Kress, Lattice dynamics of high-T_c superconductors: Optical modes of the thallium-based compounds, Phys. Rev. B **41**, 6409 (1990).

[75] K. F. McCarty, B. Morosin, D. S. Ginley, and D. R. Boehme, Raman analysis of $TlCa_2Ba_2Cu_3O_{19}$ and $Tl_2Ca_2Ba_2Cu_3O_{10}$ crystals, Physica C: Supercond. **157**, 135 (1989).

[76] K. F. McCarty, D. S. Ginley, D. R. Boehme, R. J. Baughman, and B. Morosin, Raman microprobe analysis of Tl-Ca-Ba-Cu-O polycrystals, Solid State Commun. **68**, 77 (1988).

[77] V. B. Timofeev, A. A. Maksimov, O. V. Misochko, and I. I. Tartakovskii, Light scattering spectroscopy of Tl-based superconductors: Phonon and electronic excitations, Physica C **162–164**, 1409 (1989).

[78] R. Zeyher and G. Zwicknag, Superconductivity-induced phonon self-energy effects in high-T_c superconductors, Z. Phys. B **78**, 175 (1990).

[79] E. J. Nicol, C. Jiang, and J. P. Carbotte, Effect of d-wave energy-gap symmetry on Raman shifts, Phys. Rev. B **47**, 8131 (1993).

[80] T. P. Devereaux and D. Einzel, Electronic Raman scattering in superconductors as a probe of anisotropic electron pairing, Phys. Rev. B **51**, 16336 (1995).

[81] N. L. Wang, P. Zheng, J. L. Luo, Z. J. Chen, S. L. Yan, L. Fang, and Y. C. Ma, Strong electron-boson coupling effect in the infrared spectra of $Tl_2Ba_2CaCu_2O_{8+\delta}$, Phys. Rev. B **68**, 054516 (2003).

[82] L. Ozyuzer, Z. Yusof, J. F. Zasadzinski, R. Mogilevsky, D. G. Hinks, and K. E. Gray, Evidence of $d_{x^2-y^2}$ symmetry in the tunneling conductance density of states of $Tl_2Ba_2CuO_6$, Phys. Rev. B **57**, R3245 (1998).

[83] L. Ozyuzer, Z. Yusof, J. F. Zasadzinski, T. W. Li, D. G. Hinks, and K. E. Gray, Tunneling spectroscopy of $Tl_2Ba_2CuO_6$, Physica C: Supercond. **320**, 9 (1999).

[84] Q. Huang, J. F. Zasadzinski, K. E. Gray, E. D. Bukowski, and D. M. Ginsberg, Point-contact tunneling study of the normal and superconducting states of $Tl_2Ba_2CaCu_2O_x$, Physica C: Supercond. **161**, 141 (1989).

[85] F. Giubileo, A. I. Akimenko, F. Bobba, and A. M. Cucolo, Tunneling spectroscopy and surface states in $YBa_2Cu_3O_7$ and $Tl_2Ba_2CaCu_2O_8$ break junctions, Physica C **364–365**, 626 (2001).

[86] F. Giubileo, A. Jossa, F. Bobba, A. I. Akimenko, G. Malandrino, L. M. S. Perdicaro, I. L. Fragalà, and A. M. Cucolo, Study of Andreev reflections in $Tl_2Ba_2CaCu_2O_8$/Ag interfaces, Physica C: Supercond. **367**, 170 (2002).

[87] J. S. Tsai, I. Takeuchi, Y. Shimakawa, T. Manako, and Y. Kubo, Comparison of the energy gaps in various

high-T_c oxide supercinductors, Physica C **162–164**, 1133 (1989).

[88] I. Takeuchi, J. S. Tsai, Y. Shimakawa, T. Manako, and Y. Kubo, Energy gap of Tl-Ba-Ca-Cu-O compounds by tunneling, Physica C: Supercond. **158**, 83 (1989).

[89] W. Lanping, H. Jian, and W. G. Wen, Tunneling measurement of the energy gaps in the superconductors Y-Ba-Cu-O and Tl-Ba-Ca-Cu-O, Phys. Rev. B **40**, 10954 (1989).

[90] H. H. Wen, G. Mu, H. Q. Luo, H. Yang, L. Shan, C. Ren, P. Cheng, J. Yan, and L. Fang, Specific-Heat Measurement of a Residual Superconducting State in the Normal State of Underdoped $Bi_2Sr_{2-x}La_xCuO_{6+\delta}$ Cuprate Superconductors, Phys. Rev. Lett. **103**, 067002 (2009).

[91] S. H. Han, I. Bryntse, J. Axnäs, B. R. Zhao, and Ö. Rapp, Fluctuation conductivity of polycrystalline Hg, Tl-1223, Physica C: Supercond. **388–389**, 349 (2003).

[92] K. Maki, Vortex motion in superconductors, Physica **55**, 124 (1971).

[93] J. Liu, D. Fang, Z. Wang, J. Xing, Z. Du, S. Li, X. Zhu, H. Yang, and H. H. Wen, Giant superconducting fluctuation and anomalous semiconducting normal state in $NdO_{1-x}F_xBi_{1-y}S_2$ single crystals, Europhys. Lett. **106**, 67002 (2014).

[94] J. Corson, R. Mallozzi, J. Orenstein, J. N. Eckstein, and I. Bozovic, Vanishing of phase coherence in underdoped $Bi_2Sr_2CaCu_2O_{8+\delta}$, Nature (London) **398**, 221 (1999).

[95] J. W. Loram, K. A. Mirza, J. R. Cooper, and W. Y. Liang, Electronic Specific Heat of $YBa_2Cu_3O_{6+x}$ from 1.8 to 300 K, Phys. Rev. Lett. **71**, 1740 (1993).

[96] H. M. Duan, R. M. Yandrofski, T. S. Kaplan, B. Dlugosch, J. H. Wang, and A. M. Hermann, Anisotropic resistivities of $Tl_2Ba_2CuO_{6+\delta}$ single crystals with different oxygen concentrations, Physica C: Supercond. **185–189**, 1283 (1991).

[97] H. J. Kim, P. Chowdhury, S. K. Gupta, N. H. Dan, and S. I. Lee, Effect of thermodynamic fluctuations on in-plane and out-of-plane magnetoresistance of monolayer superconductor $Tl_2Ba_2CuO_{6+\delta}$, Phys. Rev. B **70**, 144510 (2004).

[98] H. M. Duan, W. Kiehl, C. Dong, A. W. Cordes, M. J. Saeed, D. L. Viar, and A. M. Hermann, Anisotropic resistivity and paraconductivity of $Tl_2Ba_2CaCu_2O_{8+y}$ single crystals, Phys. Rev. B **43**, 12925 (1991).

[99] H. J. Kim, P. Chowdhury, W. N. Kang, D. J. Zang, and S. I. Lee, Superconducting fluctuation probed by in-plane and out-of-plane conductivities in $Tl_2Ba_2CaCuO_{8+y}$ single crystals, Phys. Rev. B **67**, 144502 (2003).

[100] P. S. Wang, J. C. Williams, D. Rathanyaka, B. Hennings, D. G. Naugle, and A. B. Kaiser, Hall coefficient for oriented $Tl_2Ba_2CaCu_2O_{8+\delta}$ thin film, Phys. Rev. B **47**, 1119 (1993).

[101] Y. C. Ma, J. W. Liu, H. W. Lu, and H. L. Zheng, Out-of-plane temperature-dependent resistivity studies on Tl-based superconductors, J. Phys.: Condens. Matter **19**, 186203 (2007).

[102] J. M. Tranquada, B. J. Sternliebt, J. D. Axe, Y. Nakamurat, and S. Uchida, Evidence for stripe correlations of spins and holes in copper oxide superconductors, Nature (London) **375**, 561 (1995).

[103] J. E. Hoffman, E. W. Hudson, K. M. Lang, V. Madhavan, H. Eisaki, S. Uchida, and J. C. Davis, A four unit cell periodic pattern of quasi-particle states surrounding vortex cores in $Bi_2Sr_2CaCu_2O_{8+\delta}$, Science **295**, 466 (2002).

[104] T. Wu, H. Mayaffre, S. Krämer, M. Horvatić, C. Berthier, W. N. Hardy, R. X. Liang, D. A. Bonn, and M. H. Julien, Magnetic-field-induced charge-stripe order in the high-temperature superconductor $YBa_2Cu_3O_y$, Nature (London) **477**, 191 (2011).

[105] X. T. Zhu, Y. W. Cao, J. D. Zhang, E. W. Plummerb, and J. D. Guo, Classification of charge density waves based on their nature, Proc. Natl. Acad. Sci. USA **112**, 2367 (2015).

[106] R. Comin, A. Frano, M. M. Yee, Y. Yoshida, H. Eisaki, E. Schierle, E. Weschke, R. Sutarto, F. He, A. Soumyanarayanan, Y. He, M. Le Tacon, I. S. Elfimov, Jennifer E. Hoffman, G. A. Sawatzky, B. Keimer, A. Damascelli, Charge order driven by Fermi-arc instability in $Bi_2Sr_{2-x}La_xCuO_{6+\delta}$, Science **343**, 390 (2014).

[107] Z. Zhang, C. M. Lieber, D. S. Ginley, R. J. Baughman, and B. Morosin, Scanning tunneling microscopy and spectroscopy studies of the surface structure and electronic properties of single crystal Tl-Ba-Ca-Cu-O superconductors, J. Vac. Sci. Technol. B **9**, 1009 (1991).

[108] C. C. Tam, M. Zhu, J. Ayres, K. Kummer, F. Yakhou-Harris, J. R. Cooper, A. Carrington, and S. M. Hayden, Charge density waves and Fermi surface reconstruction in the clean overdoped cuprate superconductor $Tl_2Ba_2CuO_{6+\delta}$, Nature Commun. **13**, 570 (2022).

[109] M. Platé, J. D. F. Mottershead, I. S. Elfimov, D. C. Peets, R. X. Liang, D. A. Bonn, W. N. Hardy, S. Chiuzbaian, M. Falub, M. Shi, L. Patthey, and A. Damascelli, Fermi Surface and Quasiparticle Excitations of Overdoped $Tl_2Ba_2CuO_{6+\delta}$, Phys. Rev. Lett. **95**, 077001 (2005).

[110] H. J. Tao, Farun Lu, and E. L. Wolf, Observation of pseudogap in $Bi_2Sr_2CaCu_2O_{8+\delta}$ single crystals with electron tunneling spectroscopy, Physica C: Supercond. **282–287**, 1507 (1997).

[111] C. Renner, B. Revaz, J. Y. Genoud, K. Kadowaki, and Ø. Fischer, Pseudogap Precursor of the Superconducting Gap in under- and Overdoped $Bi_2Sr_2CaCu_2O_{8+\delta}$, Phys. Rev. Lett. **80**, 149 (1998).

[112] H. Takagi, B. Batlogg, H. L. Kao, J. Kwo, R. J. Cava, J. J. Krajewski, and W. F. Peck, Jr., Systematic Evolution of Temperature-Dependent Resistivity in $La_{2-x}Sr_xCuO_4$, Phys. Rev. Lett. **69**, 2975 (1992).

[113] B. Batlogg, H. Y. Hwang, H. Takagi, R. J. Cava, H. L. Kao and J. Kwo, Normal state phase diagram of (La, Sr)$_2CuO_4$ from charge and spin dynamics, Physica C: Supercond. **235–240**, 130 (1994).

[114] T. Jarlborg, Effects of spin phonon interaction within the CuO_2 plane of high-T_c superconductors, Physica C: Supercond. **454**, 5 (2007).

[115] W. Dmowksi, B. H. Toby, T. Egami, M. A. Subramanian, J. Gopalakrishnan, and A. W. Sleight, Short-Range Ordering due to Displacements of Thallium and Oxygen Atoms in Superconducting $Tl_2Ba_2CaCu_2O_8$ Observed by Pulsed-Neutron Scattering, Phys. Rev. Lett. **61**, 2608 (1988).

[116] Y. Koyama and H. Hoshiya, Soft phonon mode in the high-T_c superconductor Tl-Ba-Ca-Cu-O, Phys. Rev. B **39**, 7336 (1989).

[117] Y. Koyama, S. I. Nakamura, Y. Inoue, and T. Ohno, Direct observation of a structural-fluctuation enhancement in a superconducting state of $Tl_2Ba_2Ca_2Cu_3O_{10}$ by electron diffraction, Phys. Rev. B **46**, 5757 (1992).

[118] D. Mihailovic, T. Mertelj, and K. A. Müller, *a-b* plane optical conductivity in $YBa_2Cu_3O_{7-\delta}$ above and below $T^\star$, Phys. Rev. B **57**, 6116 (1998).

[119] V. V. Struzhkin and X. J. Chen, Magnon phonon coupling and implications for charge-density wave states and superconductivity in cuprates, Low Temp. Phys. **42**, 884 (2016).